Inorg. Chem. **2003**, *42*, 8716–8727

Crystal Structures and Magnetic Properties of 2,3,5,6-Tetrakis(2-pyridyl)pyrazine (tppz)-Containing Copper(II) Complexes

José Carranza,[1a,1b] Conor Brennan,[1a] Jorunn Sletten,*[,1c] Juan Modesto Clemente-Juan,[1a] Francesc Lloret,[1a] and Miguel Julve*[,1a]

Departament de Quimica Inorgànica/Instituto de Ciencia Molecular, Facultat de Química de la Universitat de València, Avda. Dr. Moliner 50, 46100 Burjassot (València), Spain, Facultad de Ciencias Químicas, Universidad Autónoma de Zacatecas, Jardín Juárez s/n, 98000 Zacatecas, México, and Department of Chemistry, University of Bergen, Allégaten 41, N-5007 Bergen, Norway

Received July 30, 2003

Four new copper(II) complexes of formula $[Cu_2(tppz)(dca)_3(H_2O)]\cdot dca\cdot 3H_2O$ (**1**), $[Cu_5(tppz)(N_3)_{10}]_n$ (**2**), $\{[Cu_2(tppz)(N_3)_2][Cu_2(N_3)_6]\}_n$ (**3**), and $[Cu(tppz)(N_3)_2]\cdot 0.33H_2O$ (**4**) [tppz = 2,3,5,6-tetrakis(2-pyridyl)pyrazine and dca = dicyanamide anion] have been synthesized and structurally characterized by X-ray diffraction methods. The structure of complex **1** is made up of dinuclear tppz-bridged $[Cu_2(tppz)(dca)_3(H_2O)]^+$ cations, uncoordinated dca anions, and crystallization water molecules. The copper–copper separation across bis-terdentate tppz is 6.5318(11) Å. Complex **2** is a sheetlike polymer whose asymmetric unit contains five crystallographically independent copper(II) ions. These units are building blocks in double chains in which the central part consists of a zigzag string of copper atoms bridged by double end-on azido bridges, and the outer parts are formed by dinuclear tppz-bridged entities which are bound to the central part through single end-on azido bridges. The chains are furthermore connected through weak, double out-of-plane end-on azido bridges, yielding a sheet structure. The intrachain copper–copper separations in **2** are 6.5610(6) Å across bis-terdentate tppz, 3.7174(5) and 3.8477(5) Å across single end-on azido bridges, and from 3.0955(5) to 3.2047(7) Å across double end-on azido bridges. The double dca bridge linking the chains into sheets yields a copper–copper separation of 3.5984(7) Å. The structure of **3** consists of centrosymmetric $[Cu_2(tppz)(N_3)_2]^{2+}$ and $[Cu_2(N_3)_6]^{2-}$ units which are linked through axial Cu···N(azido) (single end-on and double end-to-end coordination modes) type interactions to afford a neutral two-dimensional network. The copper–copper separations within the cation and anion are is 6.5579(5) Å (across the bis-terdentate tppz ligand) and 3.1034(6) Å (across the double end-on azido bridges), whereas those between the units are 3.6652(4) Å (through the single end-on azido group) and 5.3508(4) Å (through the double end-to-end azido bridges). The structure of complex **4** is built of neutral $[Cu(tppz)(N_3)_2]$ mononuclear units and uncoordinated water molecules. The mononuclear units are grouped by pairs to give a rather short copper–copper separation of 3.9031(15) Å. The magnetic properties of **1**–**4** have been investigated in the temperature range 1.9–300 K. The magnetic behavior of complexes **1** and **4** is that of antiferromagnetically coupled copper(II) dimers with $J = -43.7$ (**1**) and -2.1 cm^{-1} (**4**) (the Hamiltonian being $\hat{H} = -J\hat{S}_A\cdot\hat{S}_B$). An overall ferromagnetic behavior is observed for complexes **2** and **3**. Despite the structural complexity of **2**, its magnetic properties correspond to those of magnetically isolated tppz-bridged dinuclear copper(II) units with an intermediate antiferromagnetic coupling ($J = -37.5$ cm^{-1}) plus a ferromagnetic chain of hexanuclear double azido-bridged copper(II) units (the values of the magnetic coupling within and between the hexameric units being +61.1 and +0.0062 cm^{-1}, respectively). Finally, the magnetic properties of **3** were successfully analyzed through a model of a copper(II) chain with regular alternating of three ferromagnetic interactions, $J_1 = +69.4$ (across the double end-on azido bridges in the equatorial plane), $J_2 = +11.2$ (through the tppz bridge), and $J_3 = +3.4$ cm^{-1} (across the single end-on azido bridge).

Introduction

Nitrogen aromatic heterocyclic ligands containing the pyrazine ring such as 2,3-bis(2-pyridyl)pyrazine (dpp, **I**),[2−5] pyrazino[2,3-*f*][4,7]phenanthroline (pap, **II**),[6,7] and 1,4,5,8,12-hexaazatriphenylene (hat, **III**)[8−10] have recently been used to prepare metal complexes with paramagnetic metal ions. The two main aims of these studies are the exploration of their versatility as ligands in designing extended arrays of

* To whom correspondence should be addressed. E-mail: miguel.julve@uv.es (M.J.); Jorunn.Sletten@kj.uib.no (J.S.).

(1) (a) Universitat de València. (b) Universidad Autónoma de Zacatecas. (c) University of Bergen.

10.1021/ic030244v CCC: $25.00
Published on Web 12/03/2003

metal ions and the characterization of their ability to mediate significant magnetic interactions between the paramagnetic centers that they bridge and which are separated by more than 6 Å. The structural information concerning dpp-containing complexes shows that this molecule can adopt terminal bidentate[4,11,12] and bridging bidentate/monodentate[4,13] and bis-bidentate[2,3,5,14−16] coordination modes. The largest magnetic coupling across bridging ddp is -1.38 cm^{-1} in the copper(II) chain $[Cu(dpp)(H_2O)_2]_n(BF_4)_{2n}\cdot 2nH_2O$.[3] Only a few structures of pap-containing metal complexes are known, and in all of them, copper(II) is the metal ion and pap is bis-bidentate.[6,7] The largest value of the magnetic coupling across bridging pap is $J = -2.5$ cm^{-1} in the compound $[Cu_4(pap)_4Cl_7]_nCl_n\cdot 15nH_2O$.[7] Finally, concerning the hat molecule, although its coordination chemistry is practically unexplored, the expected bidentate,[9b] bis-bidentate,[8,9a] and tris-bidentate[9a,10,17] coordination modes have been structurally characterized for this ligand. As in the preceding pap- and dpp-bridged complexes, the magnetic coupling between copper(II) ions through bridging hat is weak and antiferrromagnetic.[9a]

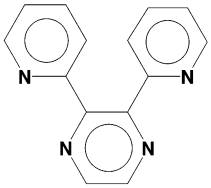

I

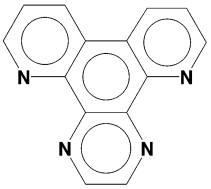

II

The poor ability of **I**−**III** to mediate magnetic interactions between the paramagnetic centers they bridge contrasts with the better efficiency of the related pyrazine derivative 2,3,5,6-tetrakis(2-pyridyl)pyrazine (tppz, **IV**), given that antiferromagnetic interactions up to -61.1 cm^{-1} were observed through the pyrazine ring of tppz in tppz-bridged copper(II) complexes.[18] It deserves to be noted that although the preparation of tppz was first reported in 1959,[19] the first structural report of a tppz-containing metal complex appeared only 10 years ago.[20] Another relevant aspect of the coordination chemistry of tppz concerns the studies of its homo- and hetero-polynuclear ruthenium complexes which have shown that tppz is an effective mediator for intermetallic coupling nearly of the order of the Creuze−Taube ion.[21−26]

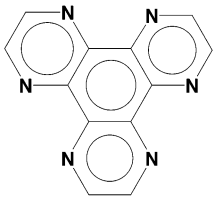

III

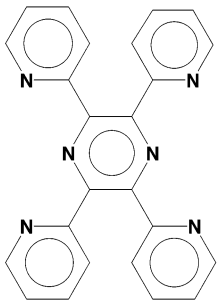

IV

In order to explore the versatility as a ligand of tppz to build extended magnetic arrays of metal ions and to get further insights on its ability to transmit magnetic interactions between the paramagnetic centers it bridges, we have undertaken a systematic study of its complex formation with first-row transition metal ions. Our first attempts afforded the copper(II) complexes of formula $[Cu_2(tppz)(dca)_3(H_2O)]\cdot dca\cdot 3H_2O$ (**1**), $[Cu_5(tppz)(N_3)_{10}]_n$ (**2**), $\{[Cu_2(tppz)(N_3)_2][Cu_2(N_3)_6]\}_n$ (**3**), and $[Cu(tppz)(N_3)_2]\cdot 0.33H_2O$ (**4**) (dca = dicyanamide anion). Their preparation, crystal structure determination, and magnetic investigation are reported here.

Experimental Section

Materials. Tppz was prepared as previously reported[19] whereas copper(II) nitrate trihydrate and the sodium salts of azide and dicyanamide were purchased from commercial sources and used as received. Elemental analyses (C, H, N) were performed by the Servicio de Microanálisis de la Universidad Complutense de Madrid.

Caution. Azide-containing complexes are potentially explosive! Only a small amount of material should be prepared, and it should be handled with care.

(2) Sletten, J.; Bjørsvik, O. *Acta Chem. Scand.* **1998**, *52*, 770.
(3) Grove, H.; Sletten, J.; Julve, M.; Lloret, F.; Lezama, L. *Inorg. Chim. Acta* **2000**, *310*, 217.
(4) Grove, H.; Julve, M.; Lloret, F.; Kruger, P. E.; Törnroos, K. W.; Sletten, J. *Inorg. Chim. Acta* **2001**, *325*, 115−124.
(5) Grove, H.; Sletten, J.; Julve, M.; Lloret, F. *J. Chem. Soc., Dalton Trans.* **2001**, 2487.
(6) Grove, H.; Sletten, J.; Julve, M.; Lloret, F. *J. Chem. Soc., Dalton Trans.* **2000**, 515.
(7) Grove, H.; Sletten, J.; Julve, M.; Lloret, F.; Cano, J. *J. Chem. Soc., Dalton Trans.* **2001**, 259.
(8) Galán-Mascarós, J. R.; Dunbar, K. *Chem. Commun.* **2001**, 217.
(9) (a) Grove, H.; Sletten, J.; Julve, M.; Lloret, F. *J. Chem. Soc., Dalton Trans*. **2001**, 1029. (b) Grove, H., Sletten, J.; Julve, M.; Lloret, F.; Lezama, L.; Carranza, J.; Parsons, P.; Rillema, P. *J. Mol. Struct.* **2002**, *606*, 253.
(10) Marshall, S. R.; Rheinhold, A. L.; Dawe, L. N.; Shum, W. W.; Kitamura, C.; Miller, J. S. *Inorg. Chem.* **2002**, *41*, 3599.
(11) Brooks, K. T.; Finnen, D. C.; Kirchhoff, J. R.; Pinkerton, A. *Acta Crystallogr*. **1994**, *C50*, 1696.
(12) Ferrari, M. B.; Fava, G. G.; Pelosi, G.; Predieri, G.; Vignali, C.; Denti, G.; Serroni, S. *Inorg. Chim. Acta* **1998**, *275*−*276*, 320.
(13) Chesnut, D. J.; Kusnetzow, A.; Birge, R. R.; Zubieta, J. *Inorg. Chem.* **1999**, *38*, 2663.
(14) Morgan, L. W.; Goodwin, K. V.; Pennington, W. T.; Petersen, J. D. *Inorg. Chem.* **1992**, *31*, 1103.
(15) Yam, V. W. W.; Lee, V. W. M.; Cheung, K. K. *J. Chem. Soc., Chem. Commun.* **1994**, 2075.
(16) Yam, V. W. W.; Lee, V. W. M.; Cheung, K. K.*Organometallics* **1997**, *16*, 2833.
(17) Abrahams, B. F.; Jackson, P. A.; Robson, R. *Angew. Chem., Int. Ed.* **1998**, *37*, 2656.
(18) Graf, M.; Stoeckli-Evans, H.; Escuer, A. Vicente, R. *Inorg. Chim. Acta* **1997**, *257*, 89.
(19) Goodwin, H. A.; Lions, F. *J. Am. Chem. Soc.* **1959**, *81*, 6415.
(20) Graf, M.; Greaves, B.; Stoeckli-Evans, H. *Inorg. Chim. Acta* **1993**, *204*, 239.
(21) Ruminski, R.; Kiplinger, J.; Cockroft, T.; Chase, C. *Inorg. Chem.* **1989**, *28*, 370.
(22) Collin, J. P.; Lainé, P., Sauvage, J. P.; Sour, A. *J. Chem. Soc., Chem. Commun.* **1993**, 434.
(23) (a) Vogler, L. M.; Scott, B.; Brewer, K. J. *Inorg. Chem.* **1993**, *32*, 898. (b) Vogler, L. M.; Brewer, K. J. *Inorg. Chem.* **1996**, *35*, 818. (c) Lee, J. D.; Vrana, L. M.; Bullock, E. R.; Brewer, K. J. *Inorg. Chem.* **1998**, *37*, 3575.
(24) Hartshorn, C. M.; Daire, N.; Tondreau, V.; Loeb, B.; Meyer, T. J.; White, P. S. *Inorg. Chem*. **1999**, *38*, 3200.
(25) Metcalfe, C.; Spey, S.; Adams, H.; Thomas, J. A. *J. Chem. Soc., Dalton Trans.* **2002**, 4732.
(26) Chanda, N.; Laye, R. H.; Chakraborthy, S.; Paul, R. L.; Jeffery, J. C.; Ward, M.; Lahiri, G. K. *J. Chem. Soc., Dalton Trans.* **2002**, 3496.

Preparation of the Complexes. $[Cu_2(tppz)(dca)_3(H_2O)]\cdot dca\cdot 3H_2O$ (1). Single crystals of **1** as green octahedra were grown by slow diffusion in an H-shaped tube of aqueous solutions containing $NaN(CN)_2$ (0.50 mmol) in one arm and a mixture of $Cu(NO_3)_2\cdot 3H_2O$ (0.25 mmol) and tppz (0.10 mmol) in the other. The diffusion was complete after one month, and most of the crystals grew in the arm containing the copper(II) salt. The crystals of **1** were collected by filtration, washed with small amounts of water, and dried on filter paper. Yield: 40%. Evaporation of the mother liquor at room temperature afforded green rodlike crystals of formula $[Cu(tppz)(dca)_2]$ which were not suitable for X-ray diffraction. Anal. Calcd for $C_{32}H_{24}Cu_2N_{18}O_4$ (**1**): C, 45.14; H, 2.82; N, 29.60. Found: C, 45.02; H, 2.75; N, 29.49.

$[Cu_5(tppz)(N_3)_{10}]_n$ (2), $\{[Cu_2(tppz)(N_3)_2][Cu_2(N_3)_6]\}_n$ (3), and **$[Cu(tppz)(N_3)_2]\cdot 0.33H_2O$ (4).** Single crystals of **2** as dark green needles (**2**) were grown by slow diffusion in an H-shaped tube of aqueous solutions containing NaN_3 (0.60 mmol) in one arm and a mixture of $Cu(NO_3)_2\cdot 3H_2O$ (0.30 mmol) and tppz (0.10 mmol) in the other. The crystals of **2** were filtered from the solution and dried on filter paper. Yield (on the basis of tppz): 50% (**2**). Slow evaporation of the mother liquor at room temperature afforded single crystals of **3** and **4** as dark green rhombohedra (**3**) and light brownish thin plates (**4**), the yield being ca. 25% for both compounds. Anal. Calcd for $C_{24}H_{16}Cu_5N_{36}$ (**2**): C, 25.60; H, 1.42; N, 44.76. Found: C, 25.48; H, 1.21; N, 44.65. Anal. Calcd for $C_{24}H_{16}Cu_4N_{30}$ (**3**): C, 29.46; H, 1.64; N, 42.93. Found: C, 29.31; H, 1.55; N, 42.80. Anal. Calcd for $C_{24}H_{16.67}CuN_{12}O_{0.33}$ (**4**): C, 53.21; H, 3.08; N, 31.01. Found: C, 53.01; H, 2.96; N, 30.89.

All our attempts to obtain only one phase in aqueous solution by playing on the Cu(II)/tppz/N_3^- molar ratio were unsuccessful. For instance, when 5:1:10 and 1:1:2 Cu(II)/tppz/N_3^- molar ratios were used, the precipitation of the $[Cu(N_3)_2]_n$ polymer occurred in the former case whereas part of the tppz remained insoluble in the latter one.

Physical Measurements. Infrared spectra were recorded on a Bruker-IF S55 spectrophotometer as KBr pellets in the 4000−400 cm^{-1} region. The magnetic susceptibilities of polycrystalline samples of complexes **1**−**4** were performed in the temperature range 1.9−300 K with a Quantum Design SQUID susceptometer, using an applied magnetic field of 1000 G. The complex $(NH_4)_2Mn(SO_4)_2\cdot 6H_2O$ was used as a susceptibility standard. Diamagnetic corrections of the constituent atoms were estimated from Pascal's constants[27] as -422×10^{-6} (**1**), -464×10^{-6} (**2**), -420×10^{-6} (**3**), and -268×10^{-6} $cm^3\ mol^{-1}$ (**4**), per two (**1**), five (**2**), four (**3**), and one (**4**) copper atoms. A value of 60×10^{-6} $cm^3\ mol^{-1}$ was used for the temperature-independent paramagnetism of the copper(II) ion.

X-ray Data Collection and Structure Refinement. Diffraction data were collected with a Bruker-AXS SMART 2K CCD area detector diffractometer equipped with an Oxford Cryostream N_2 cooling device at 153 K (**1**, **2**, **4**) and 293 K (**3**). Crystal parameters and refinement results are summarized in Table 1. Empirical absorption corrections were carried out using *SADABS*.[28] The crystals of **1** and **4** diffracted poorly; hence, the data for **4** extend to only a 2θ of 46°, and the data of **1**, extending to 2θ of 52°, contain a large fraction of reflections weaker than $2\sigma(I)$. The structures were solved by direct (**1**, **2**, and **4**) and Patterson methods (**3**), and were refined by full-matrix least-squares based on F^2, including all reflections. All non-hydrogen atoms were anisotropically refined. Hydrogen atoms bound to carbon were included in the model at idealized positions; those of the disordered water in compound **4** could not be located. All hydrogen atoms were refined according to the riding model. The noncoordinated pyridyl nitrogen atoms in **4** were identified as nitrogen both through alternative refinements as nitrogen and carbon, respectively, and by the fact that hydrogen atoms bound to carbon were clearly seen in the Fourier difference map.

Table 1. Crystal Data and Structure Refinement for $[Cu_2(tppz)(dca)_3(H_2O)]\cdot dca\cdot 3H_2O$ (**1**), $[Cu_5(tppz)(N_3)_{10}]_n$ (**2**), $\{[Cu_2(tppz)(N_3)_2][Cu_2(N_3)_6]\}_n$ (**3**), and $[Cu(tppz)(N_3)_2]\cdot 0.33H_2O$ (**4**)

	1	**2**	**3**	**4**
empirical formula	$C_{32}H_{24}Cu_2N_{18}O_4$	$C_{24}H_{16}Cu_5N_{36}$	$C_{24}H_{16}Cu_4N_{30}$	$C_{24}H_{16.67}CuN_{12}O_{0.33}$
fw	851.77	1126.43	978.83	542.06
T/K	153	153	293	153
λ/Å	0.71073	0.71073	0.71073	0.71073
space group	$P2/n$	$P2_1/c$	$P\bar{1}$	$P\bar{1}$
a/Å	8.4621(8)	14.4981(9)	7.9898(4)	10.3624(12)
b/Å	40.687(4)	13.2267(8)	9.7407(5)	10.3730(11)
c/Å	10.4565(10)	19.1270(11)	11.8232(6)	11.3654(13)
α/deg			72.4450(10)	81.015(3)
β/deg	102.213(2)	91.5420(10)	83.6300(10)	70.970(3)
γ/deg			73.7010(10)	88.979(4)
V/Å^3	3518.6(6)	3666.5(4)	841.70	1140.0(2)
Z	4	4	1	2
ρ/Mg m^{-3}	1.608	2.041	1.931	1.579
μ/mm^{-1}	1.276	2.934	2.566	1.002
R^a [$I>2\sigma(I)$]	0.0636	0.0392	0.0304	0.0538
$R_w{}^b$ [$I>2\sigma(I)$]	0.1420	0.0985	0.0779	0.0777

^{a} $R=\sum||F_o|-|F_c||/\sum|F_o|$. ^{b} $R_w=[w(F_o^2-F_c^2)^2/w(F_o^2)^2]^{1/2}$.

Data collection and data reduction were done with the *SMART* and *SAINT* programs.[29] All other calculations were performed with the *SHELXS-97*, *SHELXL/PC*, and *XP* programs.[30] Selected bond distances and angles for **1**−**4** are listed in Tables 2 (**1**), 3 (**2**), 4 (**3**), and 5 (**4**).

Results and Discussion

Description of the Structures. $[Cu_2(tppz)(dca)_3(H_2O)]\cdot dca\cdot 3H_2O$ (1). The structure consists of dinuclear tppz-bridged $[Cu_2(tppz)(dca)_3(H_2O)]$ units (Figure 1), semicoordinated dca, and crystallization water molecules. The dinuclear units are connected through hydrogen bonding involving all the water molecules. The Cu···Cu distance across the tppz bridge is 6.5618(11) Å, a value which compares well with those observed in the tppz-bridged dinuclear copper(II) complexes $[Cu_2(tppz)Cl_4]\cdot 5H_2O$ [6.565(1) Å][18] and $[Cu_2(tppz)(H_2O)_4](ClO_4)_4\cdot 2H_2O$ [6.497(2) Å].[20] The shortest intermolecular copper−copper distance in **1** is 5.5335(14) Å [Cu(2)···Cu(2f); (f) = $-x$, $-y$, $1-z$].

The two copper atoms have to a first approximation square pyramidal coordination geometries with one dca and three tppz nitrogen atoms in the equatorial positions [Cu(1)−N(7) = 1.927(5)(5) Å, Cu(1)−N(5) = 1.962(4)(4) Å, Cu(1)−N(2) = 2.018(4) Å, Cu(1)−N(1) 2.022(4) Å; Cu(2)−N(1) = 1.940(5) Å, Cu(2)−N(6) = 1.977(4) Å, Cu(2)−N(3) = 2.008(5) Å, Cu(2)−N(4) = 2.030(5) Å]. A water oxygen

(27) Earnshaw, A. *Introduction to Magnetochemistry*; Academic Press: London, 1968.
(28) *SADABS*, version 2.03; Bruker AXS Inc.: Madison, WI, 2000.
(29) (a) *SMART*, *Data Collection Software*, version 5.054; Bruker AXS Inc.: Madison, WI, 1999. (b) *SAINT*, *Data Integration Software*, version 6.02a; Bruker AXS Inc.: Madison, WI, 2001.
(30) (a) Sheldrick, G. M. SHELXS97. *Acta Crystallogr., Sect. A* **1990**, *46*, 467. (b) Sheldrick, G. M. *SHELXTL/PC*, version 6.12; Bruker AXS Inc.: Madison, WI, 1998. (c) Sheldrick, G. M. *XP*, version 5.1; Bruker AXS Inc.: Madison, WI, 1998.

Table 2. Selected Bond Lengths (Å) and Angles (deg)[a,b] for $[Cu_2(tppz)(dca)_3(H_2O)]\cdot dca\cdot 3H_2O$ (**1**)

Copper Coordination Sphere			
Cu(1)−N(7)	1.927(5)	Cu(2)−N(10)	1.940(5)
Cu(1)−N(5)	1.962(4)	Cu(2)−N(6)	1.977(4)
Cu(1)−N(2)	2.018(4)	Cu(2)−N(3)	2.008(5)
Cu(1)−N(1)	2.022(4)	Cu(2)−N(4)	2.030(5)
Cu(1)−O(1)	2.281(4)	Cu(2)−N(13)	2.187(6)
Cu(1)−N(18)	2.939(5)	Cu(2)−O(3)	3.073(5)
N(7)−Cu(1)−N(5)	172.56(18)	N(10)−Cu(2)−N(6)	162.8(2)
N(7)−Cu(1)−N(2)	99.28(18)	N(10)−Cu(2)−N(3)	98.98(19)
N(5)−Cu(1)−N(2)	79.63(17)	N(6)−Cu(2)−N(3)	79.55(18)
N(7)−Cu(1)−N(1)	100.62(18)	N(10)−Cu(2)−N(4)	99.0(2)
N(5)−Cu(1)−N(1)	79.78(17)	N(6)−Cu(2)−N(4)	79.89(18)
N(2)−Cu(1)−N(1)	159.03(17)	N(3)−Cu(2)−N(4)	158.68(18)
N(7)−Cu(1)−O(1)	94.68(16)	N(10)−Cu(2)−N(13)	98.3(2)
N(5)−Cu(1)−O(1)	92.75(15)	N(6)−Cu(2)−N(13)	98.84(18)
N(2)−Cu(1)−O(1)	94.43(15)	N(3)−Cu(2)−N(13)	99.9(2)
N(1)−Cu(1)−O(1)	90.49(15)	N(4)−Cu(2)−N(13)	88.8(2)
N(7)−Cu(1)−N(18)	82.47(16)	N(10)−Cu(2)−O(3)	82.75(19)
N(5)−Cu(1)−N(18)	90.24(16)	N(6)−Cu(2)−O(3)	80.50(16)
N(2)−Cu(1)−N(18)	93.52(16)	N(3)−Cu(2)−O(3)	72.24(17)
N(1)−Cu(1)−N(18)	82.62(16)	N(4)−Cu(2)−O(3)	98.82(17)
O(1)−Cu(1)−N(18)	171.90(13)	N(13)−Cu(2)−O(3)	172.12(17)

Hydrogen Bonds[c]

D	A	H	D···A (Å)	H···A (Å)	D−H···A (deg)
O(1)	N(16a)	H(42)	2.840(7)	1.96	163
O(1)	N(18b)	H(41)	2.944(6)	1.96	174
O(2)	O(3)	H(44)	2.74(6)	1.68	161
O(2)	N(8b)	H(43)	3.139(7)	2.18	146
O(3)	N(11c)	H(45)	2.938(7)	1.99	170
O(3)	N(15d)	H(46)	2.844(9)	1.60	170
O(4)	N(9)	H(47)	2.945(9)	1.98	149

[a] Estimated standard deviations in the last significant digits are given in parentheses. [b] Symmetry transformations: (a) $x, y, 1 + z$; (b) $0.5 + x, 0.5 - y, 0.5 + z$; (c) $1 - x, -y, 1 - z$; (d) $1 + x, y, 1 + z$. [c] A = acceptor, D = donor.

[Cu(1)−O(1) = 2.281(4) Å] and a dca nitrogen [Cu(2)−N(13) = 2.187(6) Å] fill the apical position at Cu(1) and Cu(2), respectively. In addition, the dca counterion is semicoordinated to Cu(1) [Cu(1)−N(18) = 2.939(5) Å], while one of the crystal water molecules is semicoordinated to Cu(2) [Cu(2)−O(3) = 3.073(5) Å]. The equatorial plane of Cu(1) is close to planar (maximum atomic deviation being 0.019 Å) with Cu(1) displaced by 0.109 Å from the plane toward the apical water molecule. The equatorial plane of Cu(2) has a tetrahedral distortion (maximum atomic deviation being 0.082 Å) with Cu(2) displaced by 0.222 Å from the plane toward the apical dca ligand. The central pyrazine ring of the tppz bridge is significantly twisted (maximum atomic deviation from mean plane 0.121 Å), and its mean plane has dihedral angles of 14.0° and 15.1°, respectively, to the two copper equatorial planes. Dihedral angles between the pyrazine ring and the four pyridyl rings are 19.6°, 20.6°, 24.2°, and 24.8°, respectively. Bond distances and angles of the tppz group in **1** agree with those previously observed for this ligand exhibiting the bis-terdentate coordination mode in a few structurally characterized examples with Cu(II),[18,20] Ni(II),[18] Ru(II),[24,26] and Rh(I).[31]

$[Cu_5(tppz)(N_3)_{10}]_n$ (2). The asymmetric unit, consisting of five copper(II) ions, one tppz group, and 10 azide groups, is shown in Figure 2. These units are connected into a double chain depicted in Figure 3. The central part of this double chain features a zigzag string of copper atoms [Cu(3), Cu(4), Cu(5) as repetition unit] bridged by double end-on azido bridges. This central part is then connected through single end-on azido bridges at Cu(3) [Cu(3)−N(13)-Cu(2)] and Cu(5) [Cu(5)−N(31)-Cu(1e); (e) = $1 + x, y, z$] to the outer part of the double chain, consisting of tppz-bridged Cu(1) and Cu(2) atoms. There is an additional weak, asymmetric, end-to-end bridge between Cu(2) and Cu(4) [Cu(2)−N(10)−N(11)−N(12)···Cu(4)]. The double chains are furthermore linked through semicoordinated end-on azido groups into a sheet structure (Figure 4) [Cu(1)−N(7b) = 2.777(2) Å; (b) = $-x, 2 - y, 1 - z$]. Copper−copper distances across the double azido bridges within the chain are the following:

Table 3. Selected Bond Lengths (Å) and Angles (deg)[a,b] for $[Cu_5(tppz)(N_3)_{10}]_n$ (**2**)

Copper Coordination			
Cu(1)−N(7)	1.933(2)	Cu(3)−N(19)	2.012(2)
Cu(1)−N(5)	1.976(2)	Cu(3)−N(16c)	2.057(3)
Cu(1)−N(2)	2.002(2)	Cu(3)−N(22)	2.247(3)
Cu(1)−N(1)	2.010(2)	Cu(4)−N(22)	1.968(3)
Cu(1)−N(31a)	2.328(2)	Cu(4)−N(28)	1.974(3)
Cu(1)−N(7b)	2.777(2)	Cu(4)−N(25)	1.980(3)
Cu(2)−N(10)	1.931(2)	Cu(4)−N(19)	2.011(3)
Cu(2)−N(6)	1.972(2)	Cu(4)−N(12)	2.589(3)
Cu(2)−N(3)	2.017(2)	Cu(5)−N(34)	1.952(3)
Cu(2)−N(4)	2.018(2)	Cu(5)−N(31)	1.981(3)
Cu(2)−N(13)	2.282(2)	Cu(5)−N(28)	2.007(2)
Cu(3)−N(13)	1.973(2)	Cu(5)−N(25)	2.053(3)
Cu(3)−N(16)	1.983(3)	Cu(5)−N(34d)	2.354(3)
N(7)−Cu(1)−N(5)	160.13(10)	N(16)−Cu(3)−N(22)	96.12(11)
N(7)−Cu(1)−N(2)	94.21(10)	N(19)−Cu(3)−N(22)	77.38(10)
N(5)−Cu(1)−N(2)	80.14(9)	N(16c)−Cu(3)−N(22)	98.09(11)
N(7)−Cu(1)−N(1)	103.74(10)	N(22)−Cu(4)−N(28)	99.75(11)
N(5)−Cu(1)−N(1)	79.98(9)	N(22)−Cu(4)−N(25)	168.78(12)
N(2)−Cu(1)−N(1)	159.97(9)	N(28)−Cu(4)−N(25)	79.70(11)
N(7)−Cu(1)−N(31a)	108.16(10)	N(22)−Cu(4)−N(19)	84.26(10)
N(5)−Cu(1)−N(31a)	91.07(9)	N(28)−Cu(4)−N(19)	175.59(10)
N(2)−Cu(1)−N(31a)	91.00(10)	N(25)−Cu(4)−N(19)	96.72(10)
N(1)−Cu(1)−N(31a)	91.78(9)	N(22)−Cu(4)−N(12)	95.29(10)
N(7)−Cu(1)−N(7b)	81.96(9)	N(28)−Cu(4)−N(12)	91.73(10)
N(5)−Cu(1)−N(7b)	78.46(8)	N(25)−Cu(4)−N(12)	95.92(10)
N(2)−Cu(1)−N(7b)	83.03(9)	N(19)−Cu(4)−N(12)	86.04(10)
N(1)−Cu(1)−N(7b)	90.64(9)	N(34)−Cu(5)−N(31)	100.67(12)
N(31a)−Cu(1)−N(7b)	168.68(9)	N(34)−Cu(5)−N(28)	166.08(11)
N(10)−Cu(2)−N(6)	164.05(10)	N(31)−Cu(5)−N(28)	93.22(11)
N(10)−Cu(2)−N(3)	96.17(10)	N(34)−Cu(5)−N(25)	91.42(11)
N(6)−Cu(2)−N(3)	79.91(9)	N(31)−Cu(5)−N(25)	146.51(11)
N(10)−Cu(2)−N(4)	100.69(10)	N(28)−Cu(5)−N(25)	77.21(10)
N(6)−Cu(2)−N(4)	80.14(9)	N(34)−Cu(5)−N(34d)	84.27(11)
N(3)−Cu(2)−N(4)	158.31(9)	N(31)−Cu(5)−N(34d)	112.70(10)
N(10)−Cu(2)−N(13)	104.05(10)	N(28)−Cu(5)−N(34d)	89.64(10)
N(6)−Cu(2)−N(13)	91.43(9)	N(25)−Cu(5)−N(34d)	99.42(11)
N(3)−Cu(2)−N(13)	89.50(9)	Cu(3)−N(13)−Cu(2)	129.30(13)
N(4)−Cu(2)−N(13)	99.43(9)	Cu(3)−N(16)−Cu(3c)	100.69(12)
N(13)−Cu(3)−N(16)	95.91(11)	Cu(3)−N(19)−Cu(4)	102.00(11)
N(13)−Cu(3)−N(19)	94.67(10)	Cu(3)−N(22)−Cu(4)	95.52(11)
N(16)−Cu(3)−N(19)	169.15(11)	Cu(4)−N(25)−Cu(5)	100.28(12)
N(13)−Cu(3)−N(16c)	148.41(12)	Cu(4)−N(28)−Cu(5)	102.04(11)
N(16)−Cu(3)−N(16c)	79.31(12)	Cu(5)−N(31)−Cu(1e)	119.02(12)
N(19)−Cu(3)−N(16c)	92.88(10)	Cu(5)−N(34)−Cu(5d)	95.73(11)
N(13)−Cu(3)−N(22)	113.49(11)	Cu(1)−N(7)−Cu(1b)	98.04(9)

[a] Estimated standard deviations in the last significant digits are given in parentheses. [b] Symmetry transformations used to generate equivalent atoms: (a) $x - 1, y, z$; (b) $-x, -y + 2, -z + 1$; (c) $-x + 1, -y + 1, -z + 1$; (d) $-x + 2, -y + 1, -z + 1$; (e) $x + 1, y, z$.

(31) Bera, J. K.; Campos-Fernández, C. S.; Rodolphe, C.; Dunbar, K. R. *Chem. Commun.* **2002**, 2536.

Table 4. Selected Bond Lengths (Å) and Angles (deg)[a,b] for $\{[Cu_2(tppz)(N_3)_2][Cu_2(N_3)_6]\}_n$ (**3**)

Copper Coordination			
Cu(1)−N(4)	1.9438(19)	Cu(2)−N(10)	1.9513(19)
Cu(1)−N(3)	1.9850(16)	Cu(2)−N(7)	1.967(2)
Cu(1)−N(1)	2.023(2)	Cu(2)−N(13)	1.980(2)
Cu(1)−N(2)	2.039(2)	Cu(2)−N(13a)	1.988(3)
Cu(1)−N(12c)	2.507(3)	Cu(2)−N(6d)	2.702(4)
Cu(1)−N(7)	2.561(2)		

N(4)−Cu(1)−N(3)	170.26(8)	N(12c)−Cu(1)−N(7)	172.49(8)
N(4)−Cu(1)−N(1)	106.45(9)	N(10)−Cu(2)−N(7)	96.20(10)
N(3)−Cu(1)−N(1)	78.96(7)	N(10)−Cu(2)−N(13)	164.75(11)
N(4)−Cu(1)−N(2)	96.45(9)	N(7)−Cu(2)−N(13)	93.70(10)
N(3)−Cu(1)−N(2)	79.52(7)	N(10)−Cu(2)−N(13a)	91.60(10)
N(1)−Cu(1)−N(2)	155.87(7)	N(7)−Cu(2)−N(13a)	168.64(9)
N(4)−Cu(1)−N(12c)	87.44(8)	N(13)−Cu(2)−N(13a)	77.07(10)
N(3)−Cu(1)−N(12c)	101.38(7)	N(10)−Cu(2)−N(6d)	91.61(8)
N(1)−Cu(1)−N(12c)	83.21(9)	N(7)−Cu(2)−N(6d)	86.50(10)
N(2)−Cu(1)−N(12c)	90.44(9)	N(13)−Cu(2)−N(6d)	100.57(11)
N(4)−Cu(1)−N(7)	87.90(8)	N(13a)−Cu(2)−N(6d)	101.57(12)
N(3)−Cu(1)−N(7)	83.73(7)	Cu(2)−N(13)−Cu(2a)	102.93(10)
N(1)−Cu(1)−N(7)	92.47(8)	Cu(2)−N(7)−Cu(1)	107.36(10)
N(2)−Cu(1)−N(7)	95.94(8)		

[a] Estimated standard deviations in the last digits are given in parentheses. [b] Symmetry transformations used to generate equivalent atoms: (a) $-x+1, -y+1, -z$; (b) $-x+1, -y+1, -z+1$; (c) $x+1, y, z$; (d) $x-1, y, z$.

Table 5. Selected Bond Lengths (Å) and Angles (deg)[a] for $[Cu(tppz)(N_3)_2]\cdot 0.33H_2O$ (**4**)

Copper Coordination Sphere			
Cu(1)−N(10)	1.944(5)	Cu(1)−N(2)	2.051(4)
Cu(1)−N(5)	1.974(4)	Cu(1)−N(7)	2.141(5)
Cu(1)−N(1)	2.021(4)		

N(10)−Cu(1)−N(5)	157.63(18)	N(1)−Cu(1)−N(2)	156.21(18)
N(10)−Cu(1)−N(1)	100.80(18)	N(10)−Cu(1)−N(7)	101.1(2)
N(5)−Cu(1)−N(1)	79.17(18)	N(5)−Cu(1)−N(7)	101.15(19)
N(10)−Cu(1)−N(2)	95.96(19)	N(1)−Cu(1)−N(7)	96.68(17)
N(5)−Cu(1)−N(2)	78.91(18)	N(2)−Cu(1)−N(7)	96.53(17)

[a] Estimated standard deviations in the last significant digits are given in parentheses.

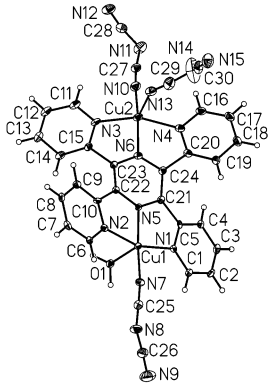

Figure 1. The complex unit in $[Cu_2(tppz)(dca)_3(H_2O)]\cdot dca\cdot 3H_2O$ (**1**). Thermal ellipsoids are plotted at the 30% probability level.

Cu(3)···Cu(4) = 3.1263(5) Å, Cu(3)···Cu(3c) = 3.1106(7) Å [(c) = $1-x, 1-y, 1-z$)], Cu(4)···Cu(5) = 3.0955(5) Å and Cu(5)···Cu(5d) = 3.2047(7) Å [(d) = $2-x, 1-y, 1-z$]. The values of the copper−copper separation across the single end-on azido bridges are the following: Cu(3)···Cu(2) = 3.8477(5) Å and Cu(5)···Cu(1e) = 3.7174(5) Å [(e) = $1+x, y, z$]. The intermetallic distance across the tppz bridge is Cu(1)···Cu(2) = 6.5610(6) Å. Finally, the

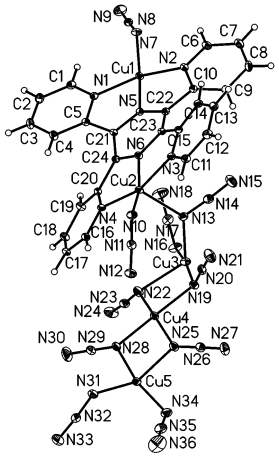

Figure 2. The asymmetric units in **2**, $[Cu5(tppz)(N_3)_{10}]_n$, including the atomic numbering scheme. Thermal ellipsoids are plotted at the 30% probability level.

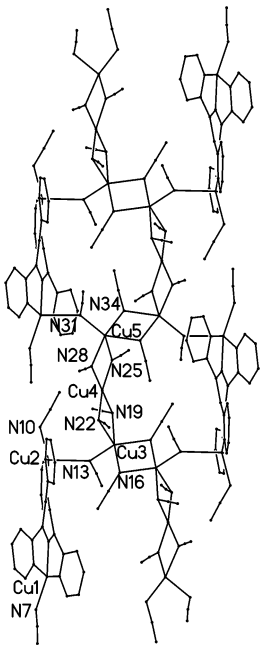

Figure 3. The double chain in $[Cu_5(tppz)(N_3)_{10}]_n$ (**2**).

interchain connection across double semicoordinated azido bridges yields a copper−copper distance of Cu(1)···Cu(1b) = 3.5984(7) Å [(b) = $-x, 2-y, 1-z$]. This is a quite unusual azido-containing metal complex where terminal (monodentate) and bridging (single and double end-on) azide groups coexist.

Including the semicoordinated azide, Cu(1) has a distorted elongated octahedral $4+1+1'$ coordination with three tppz nitrogen atoms and one azide nitrogen in equatorial positions. The equatorial plane has a significant tetrahedral distortion (maximum atomic deviation of 0.131 Å) with the copper atom displaced by 0.215 Å from this plane toward the strongest bound axial azido group. Cu(2) has a square pyramidal coordination sphere with three tppz and one azido nitrogen in equatorial positions and a single end-on azide occupying the apical site. The equatorial plane has a very minor tetrahedral distortion (maximum atomic deviation being 0.042 Å), and the copper atom is displaced by 0.232

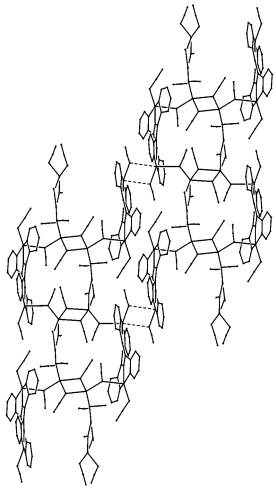

Figure 4. The sheet structure of $[Cu_5(tppz)(N_3)_{10}]_n$ (**2**).

Å toward the apical ligand. Cu(3), Cu(4), and Cu(5) are bound to only azide ligands, each being surrounded by five nitrogen atoms. While Cu(4) has a relatively close to square planar coordination, the coordination spheres of Cu(3) and Cu(5) show pronounced distortions toward trigonal bipyramidal geometry. The $Cu(4)N_4$ chromophore shows a distortion comparable to the basal plane of Cu(1) and Cu(2) [maximum atomic deviation of 0.119 Å with copper displaced by 0.077 Å]. On the basis of the square pyramidal description, the equatorial planes of Cu(3) and Cu(5) are appreciably more distorted with maximum atomic deviations of 0.335 Å in both cases, and the metal atoms displaced by 0.224 and 0.235 Å, respectively. The Cu−N−Cu bond angles at the double end-on azido bridges between Cu(3), Cu(4), and Cu(5) range from 95.52(11)° to 102.04(11)°, while the corresponding angles at the single end-on azido bridges between Cu(2)/Cu(3) and Cu(5)/Cu(1e) are 129.30(13)° and 119.02(12)°.

$\{[Cu_2(tppz)(N_3)_2][Cu_2(N_3)_6]\}_n$ (3). The building blocks of this compound may be identified as $[Cu_2(tppz)(N_3)_2]^{2+}$ and $[Cu_2(N_3)_6]^{2-}$ units (Figure 5) which are linked into a two-dimensional network structure through axial Cu···N(azide) bonds (Figure 6). In the cationic units, two centrosymmetrically related copper atoms are bridged by tppz serving as a bis-terdentate ligand. The copper has a distorted, elongated octahedral coordination geometry with three tppz and one azide nitrogen atoms in equatorial positions (Cu−N 1.944−2.039 Å) and two azide nitrogen atoms of two anions in the axial positions [Cu(1)−N(7) = 2.561(2) Å and Cu(1)−N(12c) =2.507(3) Å; (c) = 1 + *x*, *y*, *z*]. Cu(1) is shifted only 0.006 Å from the mean basal plane, but it is displaced by 0.562 Å from the pyrazine plane. The value of the dihedral angle between this equatorial plane and that of the pyrazine ring is 21.7°. In the anion, the two centrosymmetrically related copper atoms are bridged with double end-on azido bridges (Figure 5, bottom). The copper has a distorted square pyramidal coordination sphere with the equatorial positions occupied by four azide nitrogen atoms, two of these from azide groups bridging within the anion unit (Cu−N 1.951−1.988 Å). A nitrogen atom [N(6)] from a neighboring cationic

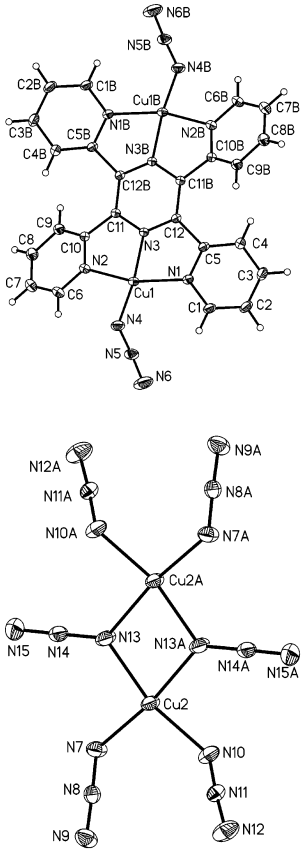

Figure 5. Perspective views of the $[Cu_2(tppz)(N_3)_2]^{2+}$ (top) and $[Cu_2(N_3)_6]^{2-}$ (bottom) units in compound **3**. Thermal ellipsoids are plotted at the 30% probability level.

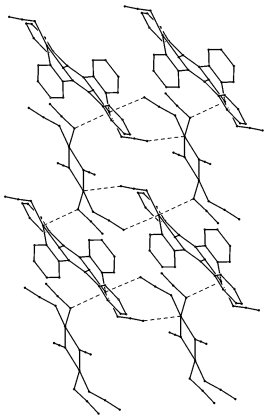

Figure 6. The sheet structure in $\{[Cu_2(tppz)(N_3)_2][Cu_2(N_3)_6]\}_n$ (**3**).

unit occupies the apical position being weakly bound to the copper atom [Cu(2)−N(6d) = 2.702(4) Å; (d) = *x* − 1, *y*, *z*). Cu(2) is shifted by 0.157 Å from the mean basal plane. The resulting sheetlike structure (Figure 6) may be described in the following way: first, alternating anions and cations are linked into chains through single end-on azide bridges [Cu(2)−N(7)···Cu(1)], and second, these chains are linked into sheets through double end-to-end azide bridges [Cu(2)−N(10)−N(11)−N(12)···Cu(1d) and Cu(2)···N(6d)−N(5d)−N(4d)−Cu(1d)]. The values of the copper−copper distance across the double end-on azide bridge within the anion [Cu(2)···Cu(2a)] and through the single end-on azide bridge between cation and anion [Cu(1)···Cu(2)] are 3.1034(6) and

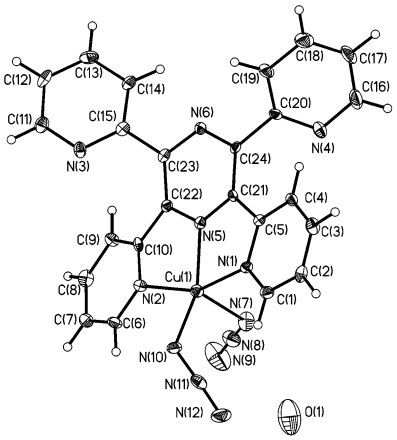

Figure 7. The molecular unit in $[Cu(tppz)(N_3)_2]\cdot 0.33H_2O$ (**4**). Thermal ellipsoids are plotted at the 30% probability level.

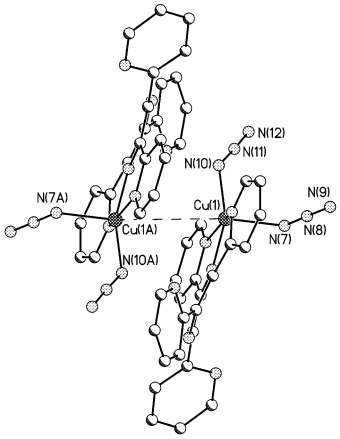

Figure 8. Two centrosymmetrically related units in $[Cu(tppz)(N_3)_2]\cdot 0.33H_2O$ (**4**), showing the short Cu···Cu(a) distance [symmetry code: (a) $-x, 1-y, 1-z$].

3.6652(4) Å, respectively. These values are shorter than the metal−metal separations across the double end-to-end azide bridge [5.3508(4) Å for Cu(2)···Cu(1d)], and the tppz bridge [6.5579(5) Å for Cu(1)···Cu(1b); (b) = $1+x, y, z$].

$[Cu(tppz)(N_3)_2]\cdot 0.33H_2O$ (4). The structure of **4** is built of mononuclear $[Cu(tppz)(N_3)_2]$ neutral units and water of hydration in a partially occupied position (Figure 7). Centrosymmetrically related molecules pack pairwise so as to give a rather short Cu···Cu(a) distance of 3.9031(15) Å (Figure 8). This is the only intermolecular metal−metal distance below 7.9 Å. Although hydrogen atoms on disordered water could not be localized, geometrical considerations suggest that there is hydrogen bonding between water and the coordinated azide nitrogen N(7) [O(1)···N(7) = 2.94(2) Å].

The copper atom has a distorted square pyramidal coordination geometry with three tppz nitrogen atoms [Cu(1)−N(5) = 1.974(4) Å, Cu(1)−N(1) = 2.021(4) Å, Cu(1)−N(2) = 2.051(4) Å], and one azide nitrogen [Cu(1)−N(10) = 1.944(5) Å] in the equatorial positions, and another azide [Cu(1)−N(7) = 2.141(5) Å] in the apical position. The sixth coordination position is screened by the proximity of a centrosymmetrically related molecule (Figure 8). The atoms defining the equatorial plane of copper have a tetrahedral distortion (maximum atomic deviation being 0.083 Å), and the metal is displaced by 0.304 Å from this plane toward the apical nitrogen. The tridentate coordination mode of tppz in **4** was previously observed in other tppz-containing complexes with Cu(II),[20] Zn(II),[20] Ru(II),[32] Ir(III).[23a] The central pyrazine ring of tppz in **4** is significantly puckered (maximum atomic deviations being 0.084 Å), the pyrazine mean plane making dihedral angles of 15.2°, 21.2°, 29.9°, and 53.0° with the pyridyl rings.

Infrared Spectra. The most significant features of the infrared spectrum of **1** appear in the high-frequency region, and they consist of a strong and broad absorption at 3440 cm^{-1} (O−H stretching of water molecules with hydrogen bonds) and four peaks at 2305m, 2240s, 2175vs, and 2155vs cm^{-1} [ν(C≡N) of the dca group].[33] The displacement and the greater number of the dca peaks in **1** as compared to those of the free dca in its sodium salt [2286s, 2232s, and 2179vs cm^{-1}] are due to the presence of monodentate and semicoordinated dca groups in **1** as revealed by its crystal structure. The presence in the IR spectra of **2**−**4** of strong peaks at 2045 and 2020 cm^{-1} (**2**), 2075, 2050, and 2040 cm^{-1} (**3**), and 2060 and 2040sh cm^{-1} (**4**) [$\nu_{as}(N_3^-)$] and their shift to lower wavenumbers with respect to free azide (a single strong absorption centered at 2133 cm^{-1} for sodium azide) indicate the coordination of azide to copper(II) in these complexes. The different coordination modes of the azide occurring in complexes **2** (terminal monodentate and single and double μ-1,1 bridges) and **3** (double μ-1,1 and single and double μ-1,3 bridges) with respect to **3** (terminal monodentate) account for the different pattern of the $\nu_{as}(N_3^-)$ stretching vibration. Although the $\nu_s(N_3^-)$ stretching is only IR active when the azido exhibits the terminal and μ-1,3-bridging mode, it has been also observed in complexes with asymmetrical μ-1,3 azido bridges.[34,35] The low intensity of these absorptions which appear around 1300 cm^{-1} and their overlap with the great number of peaks of the tppz ligand in this region preclude us to make any tentative assignment. Peaks revealing the presence of tppz in **1**−**4** occur in the ranges 3100−2900 cm^{-1} (aromatic C−H stretching vibrations), 1600−1550 cm^{-1} [ν(C═N) and ν(C═C) stretches], 1470−1020 cm^{-1} [ν(C−C) + ν(C−N) vibrations], and 810−710 cm^{-1} (aromatic C−H deformation vibrations). Some of them are somewhat shifted as compared to those of free tppz, suggesting the coordination of tppz to copper(II) in **1**−**4**. Most interestingly, an internal vibration of the pyrazine ring of tppz molecule that is located at 405m cm^{-1} in the free tppz is shifted to higher wavenumbers in **1**−**4** [468m (**1**), 445m (**2**), 465 (**3**) and 420m cm^{-1} (**4**)] because of its coordination. In light of the previous coupled spectroscopic−structural studies on pyrazine-containing copper(II) com-

(32) Tondreau, V.; Leiva, A. M.; Loeb, B. *Polyhedron* **1996**, *15*, 2035.
(33) Köhler, H.; Kolbe, A.; Lux, G. *Z. Anorg. Allg. Chem.* **1977**, *428*, 103.
(34) Nakamoto, K. *Infrared and Raman Spectra of Inorganic and Coordination Compounds*, 4th ed.; Wiley: New York, 1986; p 290.
(35) (a) Viau, G.; Lombardi, M. G.; De Munno, G.; Julve, M.; Lloret, F.; Faus, J.; Caneschi, A.; Clemente-Juan, J. M. *Chem. Commun.* **1997**, 1115. (b) Cortés, R.; Drillon, M.; Solans, X.; Lezama, L.; Rojo, T. *Inorg. Chem.* **1997**, *36*, 677.

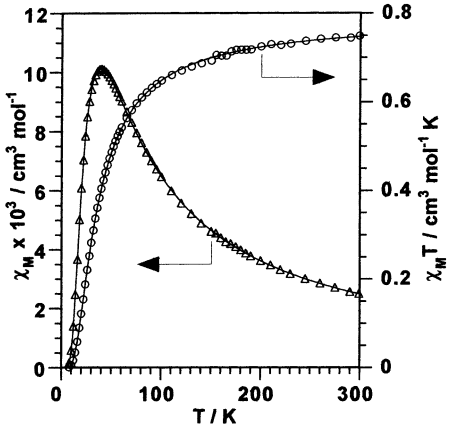

Figure 9. Thermal variation of χ_M (○) and $\chi_M T$ (△) for complex **1**. The solid line is the fit to data (see text).

plexes,[36] bridging (**1**−**3**) and terminal (**4**) pyrazine-tppz coordination modes are suggested, which are confirmed by X-ray structures.

Magnetic Properties. The magnetic properties of the compounds **1** and **4** will be discussed first because of their simplicity. Second, the magnetic properties of compound **2** will be presented and discussed. Despite the structural complexity of this compound due to the great number of exchange pathways involved [five crystallographically independen copper(II) ions], its magnetic properties were successfully modeled by introducing some simplifications which are justified on the basis of previous magneto-structural data on azido-bridged copper(II) complexes. Finally, the magnetic behavior of complex **3** will be presented and analyzed through a copper(II) chain model with regular alternating of three magnetic interactions.

The temperature dependence of χ_M and $\chi_M T$ product [χ_M is the magnetic susceptibility per two copper(II) ions] for complex **1** is shown in Figure 9. At room temperature, $\chi_M T$ is ca. 0.75 cm^3 mol^{-1} K, a value which is as expected for two spin doublets. Upon cooling, this value continuously decreases, and it vanishes at very low temperatures. The susceptibility curve exhibits a maximum at 39 K. These features are indicative of the occurrence of antiferromagnetic coupling. Taking into account the dinuclear structure of **1**, its magnetic data were analyzed through a simple Bleaney−Bowers expression for two magnetically interacting spin doublets, the Hamiltonian being $\hat{H} = -J\hat{S}_A \cdot \hat{S}_B$. The best-fit parameters obtained by least-squares fit are the following: $J = -43.7$ cm^{-1}, $g = 2.05$, and $R = 1.0 \times 10^{-5}$ (R is the agreement factor defined as $\sum_I[(\chi_M)_{obs(i)} - (\chi_M)_{calc(i)}]^2/\sum_I[(\chi_M)_{obs(i)}]^2$).

The value of the antiferromagnetic coupling in **1** ($J = -43.7$ cm^{-1}) lies between those reported for the parent tppz-bridged dinuclear copper(II) complexes of formula $[Cu_2(tppz)(H_2O)_4](ClO_4)_4 \cdot 2H_2O$ [$J = -61.1$ cm^{-1}][18,20] and $[Cu_2(tppz)Cl_4] \cdot 5H_2O$ [$J = -34.1$ cm^{-1}].[18] The exchange pathway for this significant antiferromagnetic interaction between copper(II) ions separated by ca. 6.5 Å through bridging pyrazine can be visualized through simple magnetic orbital considerations. In all three cases, the copper(II) ions are five-coordinated in a distorted square pyramidal environment, and they have three tppz-nitrogen atoms in the basal plane. Under these conditions, the unpaired electron on each copper(II) ion is described by a $d_{x^2-y^2}$ type magnetic orbital [the x and y axes being roughly defined by the Cu−N(pyrazine) and Cu−N(pyridyl) bonds]. The significant σ-overlap between the two magnetic orbitals through bridging pyrazine would account for the antiferromagnetic coupling observed in this family. A close comparison of the structures of the three compounds, focusing on the pyrazine bridging unit and the Cu−N(pyrazine) bonds, allows us to suggest which parameters may be responsible for the observed trend in the J values. In the perchlorate salt,[20] which has the strongest antiferromagnetic interaction, the pyrazine ring is essentially planar (maximum atomic deviation from the mean plane 0.012 Å), while it is significantly puckered in the other two compounds. In complex **1** the maximum deviation of the pyrazine atoms from the mean pyrazine plane is 0.121 Å, and the dihedral angle between the planes defined by C(21), N(5), C(22), and C(23), N(6), C(24) is 9.9(9)°]. In the chloride derivative,[18] the corresponding atomic deviation is 0.106 Å and the dihedral angle 11.5°. The σ in-plane overlap between the magnetic orbitals through bridging pyrazine decreases with the twisting of the pyrazine ring, and consequently, a weaker antiferromagnetic coupling is expected. The Cu−N(pyrazine) bond lengths in all the studied Cu−tppz complexes are short (significantly below 2.00 Å; refs 18, 20, and compounds **1**−**4**), compared to what is found in Cu(II) complexes bridged by the pyrazine rings of dpp, pap, and hat (significantly above 2.00 Å; refs 3−7, 9). The short Cu−N(pyrazine) bonds in the tppz bridged complexes may play an important role in yielding a much larger interaction in these cases. When comparing the perchlorate and chloride salts with **1**, it is seen that although the differences in bond lengths are very small, the shorter average distance is found in the perchlorate (Cu−N of 1.962 Å) while the longer is found in the chloride (Cu−N of 1.975 Å). A detailed theoretical study of the dependence of the magnetic coupling on pyrazine twisting, Cu−N(pyrazine) bond length, and other relevant structural parameters in tppz-bridged copper(II) dinuclear compounds has to be done once more examples are available.

The temperature dependence of the $\chi_M T$ product for complex **4** [χ_M is the magnetic susceptibility per copper(II) ion] is shown in Figure 10. At room temperature, $\chi_M T$ is equal to 0.38 cm^3 mol^{-1} K, a value which is as expected for a magnetically isolated spin doublet. It remains practically constant when cooling and decreases sharply at very low temperatures reaching a value of ca. 0.17 cm^3 mol^{-1} K at 1.86 K. The susceptibility curve exhibits an incipient maximum at 1.9 K (see inset of Figure 10). These features are indicative of the occurrence of a very weak antiferromagnetic interaction between two copper(II) ions. As shown in Figure 8, the presence of a pair of $[Cu(tppz)N_3)_2]$ units in the structure of **4** with a copper−copper separation of 3.9031(15) Å accounts for this weak magnetic interaction. Conse-

(36) Otieno, T.; Rettig, S. J.; Thompson, R. C.; Trotter, J. *Can J. Chem.* **1990**, *68*, 1901 and references therein.

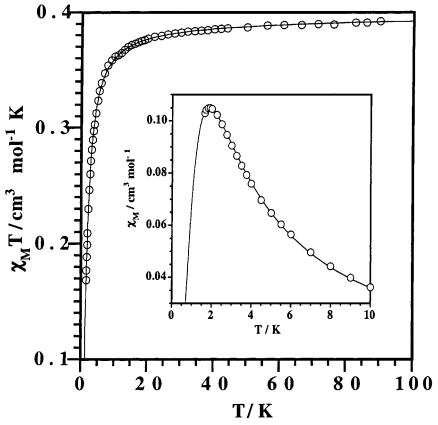

Figure 10. Thermal variation of $\chi_M T$ for complex **4**: (○) experimental data; (−) best fit curve. The inset shows the susceptibility plot in the low temperature range.

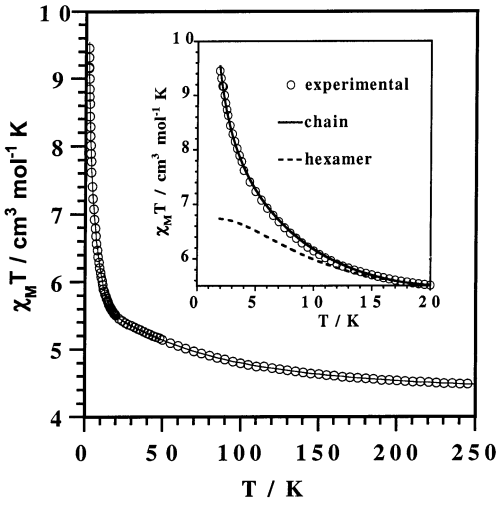

Figure 11. Thermal variation of the $\chi_M T$ product (○) for complex **2**. The solid line is the best fit to the data. The inset shows a detail of the low temperature region where the calculated curve (- - -) for the magnetically isolated hexanuclear copper(II) unit with intramolecular ferromagnetic coupling has been included for comparative purposes (see text).

quently, we have analyzed the magnetic data of **4** with the same expression used above for compound **1,** and the best-fit parameters are the following: $J = -2.07$ cm^{-1}, $g = 2.04$, and $R = 8.7 \times 10^{-6}$ (R is the agreement factor defined as $\sum_i[(\chi_M)_{obs(i)} - (\chi_M)_{calc(i)}]^2/\sum_i[(\chi_M)_{obs(i)}]^2$). This complex illustrates once more the importance of the intermolecular interactions in the magnetic studies, and it shows the need for accurate structural information when analyzing magnetic data.

The temperature dependence of the $\chi_M T$ product for complex **2** [χ_M is the magnetic susceptibility per 10 copper(II) ions] is shown in Figure 11. At room temperature, $\chi_M T$ is equal to 4.47 cm^3 mol^{-1} K, a value which is clearly above that expected for 10 magnetically isolated spin doublets (4.13 cm^3 mol^{-1} K with $g = 2.1$). Upon cooling, $\chi_M T$ smoothly increases, shows a quasi-inflection near 35 K, and then exhibits a sharp increase reaching a value of 9.50 cm^3 mol^{-1} K at 1.9 K. This curve is typical of an overall ferromagnetic interaction. The shape of the magnetization (M) versus H plot per 10 copper(II) ions of **2** at 2.0 K (see Figure 12)

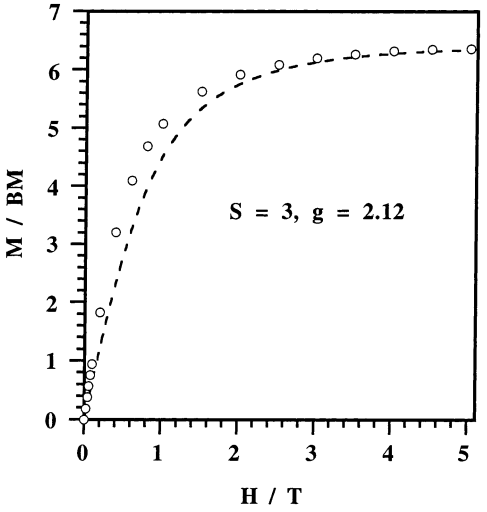

Figure 12. Magnetization versus H plot for complex **2** at 2.0 K: (○) experimental data; (- -) Brillouin function for a low lying spin state $S = 3$ with $g = 2.12$.

confirms this feature. The value of M at the maximum available magnetic field is 6.30 μ_B, and the M versus H plot lies somewhat above that of the Brillouin function for a spin state $S = 3$ with $g = 2.12$. From an inspection of Figures 11 and 12, two conclusions are evident: (i) first, six of the 10 copper(II) ions have to be ferromagnetically coupled leading to a spin state $S = 3$, with the other four copper(II) ions interacting antiferromagnetically; (ii) second, a significant ferromagnetic interaction between the $S = 3$ spin units occurs given that the values of the $\chi_M T$ product in the very low temperature range lie well above those calculated for a magnetically isolated $S = 3$ unit which would exhibit a plateau of $\chi_M T$ of ca. 6.6 cm^3 mol^{-1} K with $g = 2.1$ (see inset of Figure 11).

A careful inspection of the complicated structure of complex **2** allows us to establish a clear relationship between the magnetic properties and the crystal structure. In light of previous magneto-structural data concerning the tppz-bridged copper(II) units, the antiferromagnetic interaction corresponds to the Cu(1) and Cu(2) atoms. As far as the ferromagnetic hexanuclear unit is concerned, it most likely involves the zigzag string of copper atoms Cu(3), Cu(4), Cu(5) bridged by double end-on azido bridges. By comparing the bond distances and angles among the four double end-on azido-bridged dicopper(II) units (see **V**) and taking into account the previous magneto-structural reports on this type of motifs,[37] an identical and relatively strong ferromagnetic interaction was assumed for **V**a−c, whereas the weak ferromagnetic interaction in **V**d was discarded in a first approach. So, the ferromagnetically coupled hexanuclear unit would correspond to Cu(5c)···Cu(4c)···Cu(3c)···Cu(3)···Cu(4)···Cu(5). Keeping these considerations in mind, the susceptibility data of **2** were analyzed through the isotropic Hamiltonian [eq 1]

$$\hat{H} = -J[\hat{S}_{Cu(5c)}\cdot\hat{S}_{Cu(4c)} + \hat{S}_{Cu(4c)}\cdot\hat{S}_{Cu(3c)} + \hat{S}_{Cu(3c)}\cdot\hat{S}_{Cu(3)} + \hat{S}_{Cu(3)}\cdot\hat{S}_{Cu(4)} + \hat{S}_{Cu(4)}\cdot\hat{S}_{Cu(5)}] - J'[\hat{S}_{Cu(1)}\cdot\hat{S}_{Cu(2)} + \hat{S}_{Cu(1c)}\cdot\hat{S}_{Cu(2c)}] \quad (1)$$

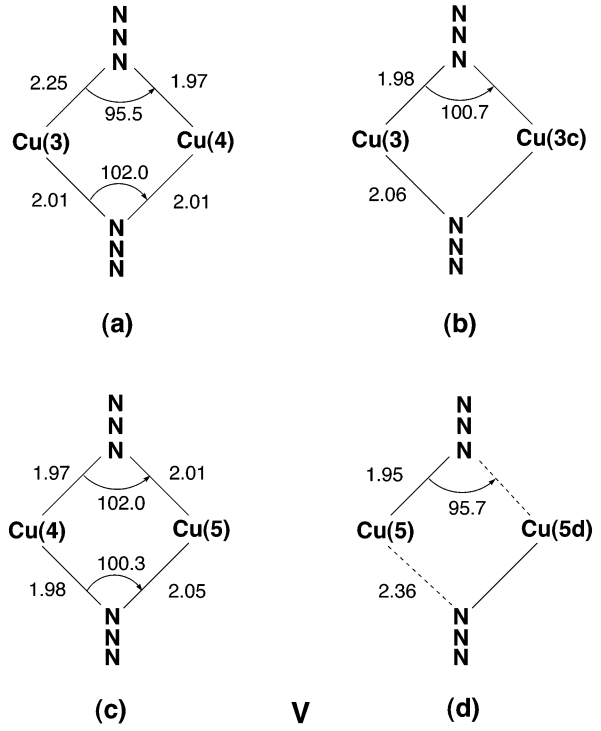

V

where J and J' are the magnetic interactions of the hexamer and dimer, respectively. Although there is no analytical expression for the magnetic susceptibility of this magnetic system, the simulation of the $\chi_M T$ versus T data was successfully performed with the MAGPACK program package.[38,39] This program allows the solution of the full Hamiltonian by a numerical procedure and the calculation of the magnetic propertiers of spin clusters of different nuclearity. The calculated curve with $J = +61.1$ cm^{-1}, $J' = -37.5$ cm^{-1}, and $g = 2.12$ matches very well the magnetic data from room temperature down to 20 K. At $T < 20$ K, the calculated curve (see inset of Figure 11) lies below the experimental one and tends to a plateau of ca. 6.70 cm^3 mol^{-1} K which would correspond to a magnetically isolated $S = 3$ spin state. This disagreement between the calculated curve and the experimental data at very low temperatures (see Figure 12) most likely has its origin in the fact that the weak ferromagnetic interaction through **V**d that we discarded above allows the hexameric units to interact each other in a ferromagnetic fashion. If this is true, the behavior of **2** in the very low temperature range could be assimilated to that of a uniform chain of repeating hexameric units which are ferromagnetically coupled. Given that at $T \leq 20$ K the spin of the hexameric unit is large enough ($S \geq 2.7$) to be considered as classic, we define an effective total spin S_{eff} of the hexamer which depends on the J/kT quotient and that is given by eq 2:[40]

$$S_{eff}(S_{eff}+1) = 8\chi_M T/g^2 \quad (2)$$

The $\chi_M T$ data of **2** at $T \leq 20$ K are analyzed through the classic spin model for a ferromagnetic linear chain with total spin S_{eff} derived by Fisher[41] [eqs 3 and 4]

$$\chi_M T = [N g_{eff}{}^2 \beta^2 S_{eff}(S_{eff}+1)/3k][(1+u)/(1-u)] \quad (3)$$

with

$$u = \coth[j_{eff} S_{eff}(S_{eff}+1)/kT] - [kT/j_{eff} S_{eff}(S_{eff}+1)] \quad (4)$$

where g_{eff} and j_{eff} stand for the Landé factor and the effective magnetic interaction between the hexameric units, respectively. The best-fit parameters are $j_{eff} = +0.0062$ cm^{-1} and $g_{eff} = 2.0$. The calculated curve reproduces very well the magnetic data at $T < 20$ K.

We would like to finish this magnetic analysis of complex **2** by a brief comment on the goodness of our crude model and the validity of the nature and magnitude of the calculated magnetic interactions J, J', and j_{eff}. It is clear that the simplicity of our model precludes the overparametrization and it provides us with a reasonable description of the magnetic properties of complex **2**. Concerning the positive value of J, this is as observed in previous magneto-structural results for this type of in-plane double end-on azido-bridged copper(II) units.[42−44] In fact, the analysis of the influence of the structural parameters on the exchange coupling constant of these compounds through DFT type calculations has shown that the value angle at the bridging azido (θ) is the most important factor,[37] a ferromagnetic interaction being predicted for $\theta < 104°$ in agreement with the experimental data. As the values of θ in **V**a−c are all below this value (mean value close to 100°), a ferromagnetic coupling is ensured, its magnitude (+61.1 cm^{-1}) being as expected. The value of the antiferromagnetic coupling between Cu(1) and Cu(2) through the tppz bridge ($J' = -37.5$ cm^{-1}) is between that of **1** (−43.7 cm^{-1}) and $[Cu_2(tppz)Cl_4]\cdot 5H_2O$ [−34.1 cm^{-1}].[18] Again this is as expected taking into account that the orientation of the magnetic orbitals in the three compounds is very close and that, in **2**, the pyrazine ring is twisted by 10.2° [value of the dihedral angle between C(21)N(5)C(22) and C(23)N(6)C(24) sets of atoms], the maximum deviation from the pyrazine ring is 0.107 Å, and the average Cu−N(pyrazine) bond length is 1.974(2) Å. Finally, the weak magnetic coupling observed through the asymmetric double end-on azido bridge in **V**d can be easily understood taking into account the out-of-plane exchange pathway involved. The magnetic orbital around each copper atom is defined by the four short equatorial bonds [N(25),

(37) Ruiz, R.; Cano, J.; Alvarez, S. *J. Am. Chem. Soc.* **1998**, *120*, 11122 and references therein.
(38) Borrás-Almenar, J. J.; Clemente-Juan, J. M.; Coronado, E.; Tsukerblat, B. S. *Inorg. Chem.* **1999**, *38*, 6081−6088.
(39) Borrás-Almenar, J. J.; Clemente-Juan, J. M.; Coronado, E.; Tsukerblat, B. S. *J. Comput. Chem.* **2001**, *22*, 985−991.
(40) (a) Lloret, F.; Ruiz, R.; Julve, M.; Faus, J., Journaux, Y.; Castro, I.; Verdaguer, M. *Inorg. Chem.* **1992**, *31*, 1150. (b) Rodríguez-Martín, Y.; Ruiz-Pérez, C.; Sanchiz, J.; Lloret, F.; Julve, M. *Inorg. Chim. Acta* **2001**, *326*, 20.
(41) Fisher, M. E. *Am. J. Phys.* **1964**, *32*, 343.
(42) Commarmond, J.; Plumeré, P.; Lehn, J. M.; Agnus, Y.; Rémy, L.; Weiss, R.; Khan, O.; Morgenstern-Badarau, I. *J. Am. Chem. Soc.* **1982**, *104*, 6330.
(43) Sikorav, S.; Bkouche-Waksman, I.; Kahn, O. *Inorg. Chem.* **1984**, *23*, 490.
(44) Tandon, S. S.; Thompson, L. K.; Manuel, M. E.; Bridson, J. N. *Inorg. Chem.* **1994**, *33*, 5555.

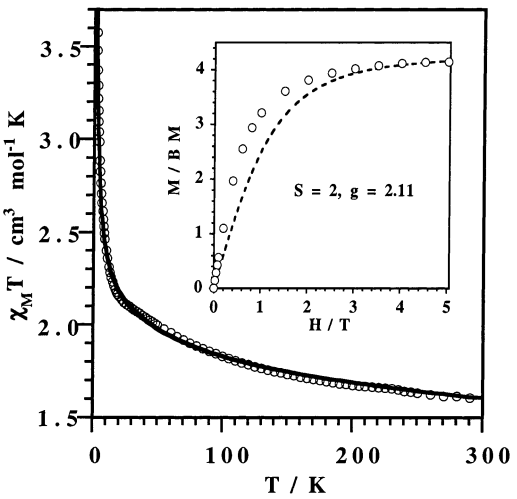

Figure 13. Thermal variation of the $\chi_M T$ product for complex **3**: (○) experimental data; (—) calculated curve (see text). The inset shows the magnetization versus H plot at 2.0 K: (○) experimental data; (- - -) Brillouin function for a magnetically isolated S = 2 spin state with $g = 2.11$.

N(28), N(31), and N(34) at Cu(5)], and it has a weak spin density on the axial position [N(34d)]. The overlap between the two parallel magnetic orbitals at Cu(5) and Cu(5d) is predicted to be very small, and under these conditions, the magnetic coupling is expected to be very weak and either ferro- or antiferromagnetic.[4]

The temperature dependence of the $\chi_M T$ product for complex **3** [χ_M is the magnetic susceptibility per four copper(II) ions] is shown in Figure 13. At room temperature, $\chi_M T$ is ca. 1.65 cm^3 mol^{-1} K, a value which is slightly above that predicted for four magnetically isolated spin doublets. On cooling, $\chi_M T$ continuously increases, shows an incipient plateau between 40 and 25 K ($\chi_M T$ tends to 2.25 cm^3 mol^{-1} K), and then exhibits an abrupt increase to reach a maximum value of 3.58 cm^3 mol^{-1} K at 2.0 K. The shape of this curve is typical of an overall ferromagnetic coupling. The magnetization (M) versus H plot per four copper(II) ions of **3** at 2.0 K (see inset of Figure 13) confirms this feature. The value of M at the maximum available magnetic field is 4.22 μ_B, and the magnetization data lie well above that of a Brillouin function for a spin state $S = 2$ with $g = 2.11$. Two conclusions are thus evident from Figure 13: (i) the four copper(II) ions are ferromagnetically coupled, and (ii) the resulting S = 2 spin state also interacts in a ferromagnetic manner as demonstrated by the value of the $\chi_M T$ at 2.0 K (3.58 cm^3 mol^{-1} K) which exceeds that calculated for a magnetically isolated $S = 2$ spin state with $g = 2.11$ (a plateau with $\chi_M T = 3.34$ cm^3 mol^{-1} K).

The interpretation of this magnetic behavior requires a detailed inspection of the structure because of the different exchange pathways which may be involved. In the structure of **3**, one can see two types of dinuclear copper(II) units, one with the bis-terdentate tppz ligand [Cu(1)···Cu1b)] and the other with the double end-on azide bridges [Cu(2)···Cu(2a)] which are linked through single asymmetric end-on azide bridges [Cu(2)−N(7)···Cu(1)] to form a chain of regular alternating tppz- and bis-μ-1,1-azido-bridged copper(II) units. These chains are further interconnected through asymmetric double end-to-end azido bridges [Cu(2)−N(10)−N(11)−N(12)···Cu(1d) and Cu(2)···N(6d)−N(5d)−N(4d)−Cu(1d)] into a sheetlike polymer. Consequently, four exchange pathways could be involved, one through the tppz molecule and three through the azido bridges. Keeping in mind that the magnetic orbital of the two copper(II) ions in **3** is defined by the four short equatorial bonds [equatorial plane built by N(1), N(2), N(3), and N(4) at Cu(1) and by N(7), N(10), N(13), and N(13a) at Cu(2)], a very weak magnetic coupling is predicted through the long axial N(12)···Cu(1d) and N(6d)···Cu(2) contacts (parallel magnetic orbitals with a copper−copper separation of 6.5579(5) Å). These considerations allow us to discard this exchange pathway, and the situation we are faced with would correspond to the following copper(II) chain (**VI**)

$$\begin{array}{l} J_1\ \ J_3\ \ J_2\ \ J_3\ \ J_1\ \ J_3\ \ J_2\ \ J_3\ \ J_1\ \ J_3\ \ J_2\ \ J_3\ \ J_1\ldots \\ \text{-}\ldots..\text{A-A}\ldots\ldots..\text{B-B}\ldots\ldots\text{A-A}\ldots\ldots\text{B-B}\ldots\ldots\text{A-A}\ldots\ldots\text{B-B}\ldots...\text{A-A}\ldots\text{-} \end{array} \quad \textbf{(VI)}$$

where J_1, J_2, and J_3 correspond to the magnetic coupling through di-μ-1,1-azido, μ-tppz, and single μ-1,1-azido bridges, respectively. There is no analytical expression for this type of copper(II) chain. This is why in order to fit its magnetic data, we have used a numerical approach which consists of modeling the chain with rings of increasing size with local spin doublets.[45,46] Sixteen interacting copper(II) ions is the upper limit in our calculations, but there is no significant difference between the fits through rings of 12 and 16 spin doublets. The values of the best-fit parameters are the following: $J_1 = +69.4$ cm^{-1}, $J_2 = +11.2$ cm^{-1}, $J_3 = +3.4$ cm^{-1}, $g = 2.11$, and $R = 1.8 \times 10^{-5}$ (R is the agreement factor defined as $\sum_i[(\chi_M T)_{obs(i)} - (\chi_M T)_{calc(i)}]^2/\sum_i[(\chi_M T)_{obs(i)}]^2$). The calculated curve matches very well the magnetic data in the whole temperature range.

Let us analyze the reliability of these best-fit values. A significant ferromagnetic coupling is expected between Cu(2) and Cu(2a) through the di-μ-1,1-azido bridge (A−A unit in **VI**) in light of previous magneto-structural results for this type of in-plane azido-bridged copper(II) units.[37,42−44] A ferromagnetic interaction is predicted for $\theta < 104°$ (θ is the value of the angle at the bridging azido).[37] As the value of θ in the double end-on azido bridged dinuclear copper(II) unit in **3** is 102.93(10)°, the ferromagnetic coupling is ensured. For the sake of comparison, a ferromagnetic interaction of ca. +70 cm^{-1} was reported for the dinuclear copper(II) complex [Cu$_2$(C$_{16}$H$_{34}$N$_2$O$_6$)(N$_3$)$_4$(H$_2$O] with θ ca. 103°.[42] Consequently, the value of $J_1 = +69.6$ cm^{-1} is in excellent agreement with that predicted. The ferromagnetic coupling through the pyrazine ring (B−B unit in **VI**) is at first sight surprising given that the magnetic coupling in the three magneto-structurally characterized tppz-bridged copper(II) dinuclear complexes is antiferromagnetic: $J = -43.7$, -34.1, and -61.1 cm^{-1} for **1**, [Cu$_2$(tppz)Cl$_4$]·5H$_2$O[18] and [Cu$_2$(tppz)(H$_2$O)$_4$](ClO$_4$)$_4$·2H$_2$O,[18,20] respectively. Although

(45) Borrás-Almenar, J. J.; Coronado, J.; Curély, J.; Georges, R.; Gianduzzo, J. *Inorg. Chem.* **1994**, *33*, 5171.
(46) De Munno, G.; Julve, M.; Lloret, F.; Faus, J.; Verdaguer, M.; Caneschi, A. *Inorg. Chem.* **1995**, *34*, 157.

the pyrazine ring is essentially planar in **3** (maximum atomic deviation from the mean plane 0.008 Å), like in the perchlorate salt, the value of the dihedral angle between the pyrazine plane and the equatorial plane of Cu(1) in **3** is 21.7°, that is nearly the double of that observed in the perchlorate compound. Having in mind the strong decrease of the antiferromagnetic interaction in the tppz-bridged dicopper(II) family which is mainly caused by the twisting of the pyrazine ring, one can assume that this distortion in **3** decreases the overlap between the magnetic orbitals and a weak ferromagnetic coupling could result. Theoretical calculations on tppz-bridged copper(II) complexes (which are beyond the goal of the present contribution) will be carried out to clarify this point when a more complete set of examples and distortions is available in the near future. Finally, the weaker ferromagnetic interaction, $J_3 = +3.4$ cm^{-1} (magnetic coupling between A−A and B−B in **VI**), corresponds to the out-of-plane single end-on azido bridge. Although magneto-structural studies of copper(II) dimers with such a single bridge are unknown, a few examples with two of these bridges have been reported, and the magnetic coupling is quite weak and ferro- or antiferromagnetic depending mainly on the value of the angle at the bridging azido-nitrogen and that of the axial copper to azido-nitrogen bond.[4] The interpretation of the weak coupling through this out-of-plane exchange pathway is straightforward. The unpaired electron of each copper(II) ion [Cu(1) and Cu(2)] is roughly defined by the four short equatorial bonds ($d_{x^2-y^2}$ type magnetic orbital), and it follows that they are in parallel planes separated by more than 3.6 Å. The small admixture of d_{z^2} accounts for the weak overlap density between the magnetic orbitals and then for a weak antiferromagnetic coupling. However, for certain values of the angle at the apical position, this overlap can vanish (accidental orthogonality), and a weak ferromagnetic coupling is observed.

Conclusion

This work shows the versatility of the tppz as ligand with tridentate (**4**) and bis-terdentate (**1**−**3**) coordination modes and its ability to transmit significant magnetic interactions between the copper(II) ions separated by more than 6.5 Å. Structural factors such as the deviations from the planarity of the pyrazine ring, the Cu−N(pyz) bond distance, and the dihedral angle between the equatorial plane of the copper atom and that of the pyrazine ring would account for the variation of the magnitude and nature (antiferro- and ferro-) of the magnetic interaction between copper(II) ions across ttpz. The influence of these factors will be clarified through DFT type calculations when a larger number of magneto-structurally characterized examples of tppz-bridged copper(II) complexes are available. The diversity of the bridging modes of the azido ligand (single and double μ-1,1 and single and double μ-1,3) and its ability to mediate ferromagnetic interactions are exemplied by the structural complexity of the layered compounds **2** and **3** who exhibit an overall ferromagnetic behavior. Only through the accurate structural knowledge of **2** and **3** was it possible to interpret their interesting and quite complicated magnetic properties. Finally, the relevance of the intermolecular interactions is well illustrated by complex **4** who exhibits a weak but significant antiferromagnetic interaction despite its mononuclear nature.

Acknowledgment. Thanks are due to NFR (research Council of Norway) and the University of Bergen for grants allowing the purchase of X-ray equipment and the Spanish Ministry of Science and Technology the European Union for financial support through the project BQU2001-2928. Three of us (J.C., C.B., and J.M.C-J.) acknowledge the Mexican Government for a predoctoral fellowship (J.C.) through the PROMEP Program, the European Union for a postdoctoral grant (C.B.) through the TMR Program Contract ERBFMRXCT-98081, and the Ministerio Español de Ciencia y Tecnología for a Ramón y Cajal contract (J.M.C-J.).

Supporting Information Available: X-ray crystallographic file, in CIF format. This material is available free of charge via the Internet at http//pubs.acs.org.

IC030244V